Local-interference theory of conductance fluctuations in ballistic metallic point contacts: Combination of near and remote backscattered trajectories

V. I. Kozub,* J. Caro, and P. A. M. Holweg†
Delft Institute of Microelectronics and Submicron Technology, Delft University of Technology, Lorentzweg 1, 2628 CJ Delft, The Netherlands
(Received 13 May 1994)

We present a theory to describe conductance fluctuations in ballistic metallic point contacts. The theory is based on interference of electron waves backscattered to the constriction of the device. Since the number of scattering events in a backscattered trajectory is small, the concept of local interference can be applied to make a first-principles calculation of the interference effect in the framework of wave optics. In the theory three different limits can be distinguished, depending on whether there is interference of remote trajectories, of near trajectories, or of a remote and a near trajectory. Interference of near trajectories leads to the estimate of Holweg *et al.* based on the Landauer formula, which for the amplitude of the fluctuations δG agrees with the experiments of these authors, but which cannot properly account for the characteristic magnetic-field scale B_c. Interference of remote trajectories, on the other hand, reproduces the result of Maslov *et al.*, also based on the Landauer formula, which can explain B_c, but which predicts a much too small δG. Finally, a combination of near and remote trajectories leads to the proper description of the experimental data. The remote trajectory, which spreads over a region of the size of the elastic mean free path, controls B_c of the fluctuations, while the near trajectory causes a substantial enhancement of δG above the value predicted by Maslov *et al.* Very good agreement with the experiments is obtained by taking into account enhanced scattering close to the constriction (a likely effect for the type of contacts studied), which gives an additional enhancement of δG. In this way, our theory successfully predicts both the value of δG and B_c in a self-consistent way, lifting previous contradictions.

I. INTRODUCTION

Recently, two of the authors reported studies of conductance fluctuations of three-dimensional (3D) nanofabricated Ag point contacts.[1,2] These aperiodic reproducible fluctuations were measured either by sweeping the magnetic field or the bias voltage. In appearance the fluctuations are very similar to universal conductance fluctuations (UCF), which occur in the diffusive transport regime.[3] The point contacts, however, are *ballistic* devices, so that the very observation of the fluctuations was quite surprising. For the devices studied, the fluctuation amplitude δG is about two order of magnitude lower than that of UCF ($\approx e^2/h$), and depends on the parameters of the point contact. An interesting property of the fluctuations is that the characteristic magnetic-field scale is given by $B_c \approx (h/e)/l_e^2$,[1,2,4] where l_e is the elastic mean free path. So, for the fluctuations observed, the role of l_e corresponds to that of the phase-coherence length for UCF. Meanwhile, magnetoconductance fluctuations have also been observed in ballistic Au and Al point contacts.[4] To demonstrate that the fluctuations are a general phenomenon in point contacts, we show in Fig. 1 fluctuation traces for Ag, Au, and Al. The ballistic devices from which these traces were taken, were made using the nanofabrication process described previously.[1,2,5] A schematic cross section of a nanofabricated point contact is shown in Fig. 2.

The explanation for the fluctuations is quantum interference of electron waves backscattered to the contact by elastic scatterers (impurities) in the electrodes or "banks" of the devices.[1,2] A simple estimate of the fluctuation amplitude can be made based on the Landauer formula using an argument of Lee,[6] by assuming that the conductance fluctuations are determined solely by the propagating electron channels in the constriction of the device and that backscattering is dominated by near scatterers. The experimental fluctuation amplitudes are in agreement with this estimate. However, there is a disagreement between the assumptions underlying the estimate and the interference loop size deduced from the experimental magnetic-field scale.

On the other hand, recently Maslov, Barnes, and Kirczenov[7] have made first-principle calculations, also based on the Landauer formula, of conductance fluctuations of a defect-free ballistic point contact between remote disordered reservoirs. In this work, also the electron channels in the scattering surrounding were taken into account. The result, however, predicts a fluctuation amplitude about two orders of magnitude smaller than observed. Thus, the theoretical situation so far can be summarized by stating that the two existing estimates of δG are mutually contradictory, and do not completely agree with the experimental picture. This makes a more profound analysis of the problem necessary.

In this paper, we present a new theoretical approach to conductance fluctuations in ballistic metallic point contacts, using the concept of "local" interference and taking

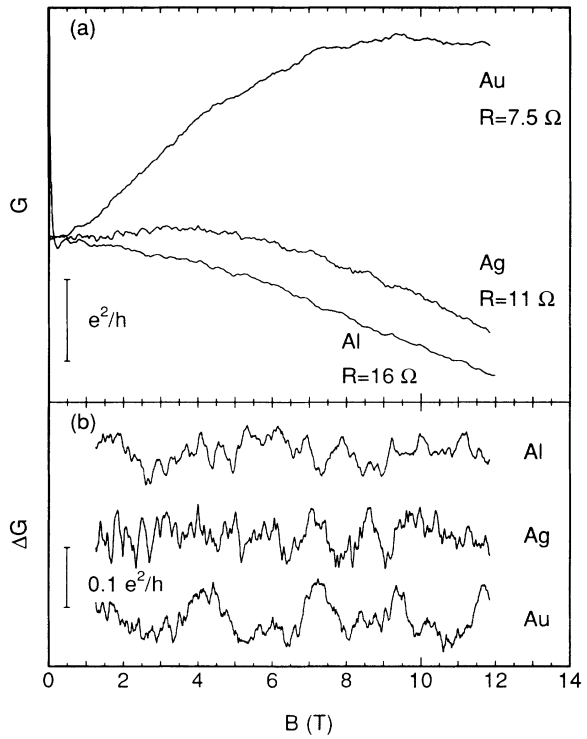

FIG. 1. Panel (a) shows magnetoconductance traces of three ballistic point contacts made of Ag, Au, and Al. The magnetic field is oriented parallel to the axis of the devices. Panel (b) shows the fluctuation traces after subtraction of the background.

into account both near and remote backscattered trajectories. Local interference (LI) describes interference of electron waves in the (quasi-)ballistic regime. On the contrary, "global" interference applies to diffusive transport,[3] the typical regime of UCF. Since the elastic mean free path l_e is much larger than the contact diameter $2a$ and comparable to the thickness of the banks, LI is the appropriate mechanism for our point contacts. Local interference enables a first-principle approach of the problem in the framework of general wave optics, providing an intuitive and simple physical picture, and agrees with the limit of a small number of scatterers of the model of Ref. 7. The concept of LI was introduced by Martin[8] to describe scattering by complex defects. Pelz and Clarke[9] used the calculations of Martin to interpret $1/f$ noise in metal films in terms of the mechanism of LI. Mesoscopic effects in bulk samples due to a generalized type of LI were discussed by Gal'perin and Kozub.[10] Also, for ballistic point contacts defined in the 2D electron gas of a

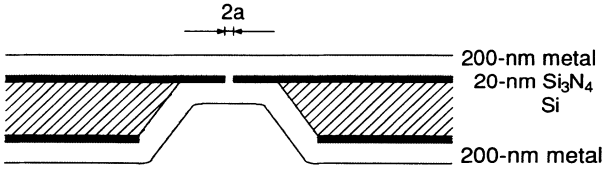

FIG. 2. Schematic cross section of a nanofabricated point contact. The diameter $2a$ of a typical point contact is in the range 5–30 nm.

GaAs heterostructure the limit of a few scatterers has been considered, in particular in relation to conductance quantization and Aharonov-Bohm oscillations (see, e.g., Refs. 11–13). However, contrary to remote scatterers discussed in the present work, in Refs. 11–13, typically one or a few scatterers inside or in close vicinity of the constriction are considered, while the effect of scattering is calculated using methods other than the wave-optical approach presented here.

This paper is organized as follows. In Sec. II, we will summarize the estimates of the fluctuation amplitude δG given in Refs. 1,7. In Sec. III, we will formulate our theory of local interference in point contacts. The main result of this section is that a combination of near and remote backscattered trajectories leads to interference which properly describes the experimental data, both for δG and B_c. This is demonstrated in two steps. First, it is found that for a homogeneous distribution of scatterers, which is assumed in Ref. 1 throughout the device and in Ref. 7 in the reservoirs, this crucial combination of trajectories gives an estimate for δG in between the estimates of Refs. 1,7, while B_c as a result of the extent of the remote trajectory has the proper magnitude. Second, we demonstrate that the plausible assumption of much stronger scattering close to the constriction than in remote regions (e.g., due to scattering at the boundary of the constriction) in case of the combination of near and remote trajectories leads to complete agreement of our theory with the experimental data. To demonstrate the universality of the wave-optical approach, we start Sec. III with showing that the estimates of Refs. 1,7 can also be obtained as limiting cases of our theory, by taking into account only near scattering or only remote scattering, respectively. In Sec. IV we summarize and conclude. In Appendix A a correlation of interference contributions of different $\mathbf{k}$ modes is discussed, while in Appendices B and C details are given of the estimates presented in the paper.

II. EXISTING ESTIMATES OF δG

A. Estimate based on the argument of Lee

The amplitude δG of the conductance fluctuations in a ballistic point contact can be obtained[1] from a modification of the argument given by Lee[6] to estimate δG for UCF. The starting point is the Landauer formula[14] for the conductance $G=(2e^2/h)\Sigma|t_{\alpha\beta}|^2$, where $|t_{\alpha\beta}|^2$ is the transmission probability of an incoming channel α to an outgoing channel β and the summation is over the number of channels $N=a^2k_F^2/4$ (k_F is the Fermi wave vector). In estimating δG, fluctuations $\delta|t_{\alpha\beta}|^2$ are considered, and transmission probabilities $|t_{\alpha\beta}|^2$ are transformed to reflection probabilities $|r_{\alpha\beta}|^2=1-|t_{\alpha\beta}|^2$ to avoid correlations among transmitted channels.[6] This gives $\delta G=(2e^2/h)N\langle|r_{\alpha\beta}|^2\rangle$, where $\langle\ \rangle$ denotes ensemble averaging. In this stage, the point-contact properties are taken into account by noting[1] that $\langle G\rangle=1/R_p=(2e^2/h)N^2\langle|t_{\alpha\beta}|^2\rangle=(1-0.82a/l_e)/R_s$. Here, R_p is the point-contact resistance given by the Wexler formula,[15] which takes into account both the

diffusive part of the resistance and the ballistic Sharvin resistance R_s. The Sharvin resistance is given by $R_s^{-1}=(2e^2/h)N$. The quantity $0.82a/l_e$ in the expression for $\langle G \rangle$ is the total probability that injected electrons are backscattered to the orifice as a result of elastic scattering. The final result of the derivation is the rms amplitude of the sample-to-sample fluctuations:

$$\delta G \approx 1.6 \frac{a}{l_e} \frac{e^2}{h} , \tag{1}$$

with Eq. (1). The fluctuations traces of Fig. 1 demonstrate this agreement (see also the discussion in Sec. III B).

Some comments in relation to Eq. (1) are in place. First, the number of channels assumed in the Landauer formula corresponds to the size of the constriction. This assumption is only valid for the immediate vicinity of the contact. Second, it is assumed that the transmission probability $\langle |t_{\alpha\beta}|^2 \rangle$ follows from the total backscattering probability. Insight in how this probability depends on the distance R of the scatterer to the contact can be obtained as follows. The probability of backscattering of an electron to the contact is of order $(\sigma/R^2)(a^2/R^2) \propto R^{-4}$, the product of the solid angle at which the scatterer is seen from the contact (σ is the cross section of the scatterer) and the solid angle at which the contact is seen from the scatterer. The total number of scatterers within radius R is $\approx N_i R^3$, where N_i is the (homogeneous) density of scatterers. So, the total backscatter probability is $(\sigma a^2/R^4)N_i R^3 = N_i \sigma a^2/R$. This probability is dominated by scatterers close to the constriction. Taking $R \approx a$ and using $N_i \sigma = l_e^{-1}$, one recovers a/l_e as total backscatter probability. As a result of the two underlying assumptions, Eq. (1) is actually limited to interference loops of size a instead of l_e. Thus, while Eq. (1) is in agreement with the observed magnitude of the fluctuations, due to the very way of its derivation there seems to be a contradiction with another experimental fact–viz. that the characteristic length scale is l_e. The conclusion is that a new theoretical model is needed, which takes into account remote scattering at distances l_e from the contact.

B. Calculation of Maslov *et al.*

Remote scattering in a point contact is treated in a recent paper of Maslov, Barnes, and Kirczenov.[7] These authors calculate δG of a defect-free ballistic point contact, connected to disordered reservoirs. The type of contact considered by the authors is defined in a 2D electron gas, but the results can also be applied to 3D point contacts. δG is calculated from the Landauer formula. The importance of this study is that in calculating the fluctuations, point contact and reservoirs are not viewed as a network of classical resistors in series, but are treated on equal footing. This is necessary, since the magnitude of the phase-coherence length extends from the constriction into the reservoirs.

The main result of Ref. 7 for the "dilute" regime (when the size of the reservoirs is smaller than the elastic mean free path) is $\delta G \approx (n/N)e^2/h$, where n and N are the number of propagating channels in the constriction and in the reservoirs, respectively. Translating this to our 3D point contacts, we get $\delta G \approx (a^2/l_e^2)e^2/h$, where N was taken as $k_F^2 l_e^2$. This result is two orders of magnitude smaller than observed experimentally. The reason is that the probability for an electron to return to the orifice from the remote region is very small. This result of Ref. 7 and the conclusion of Sec. II A lead us to the formulation of a theory of local interference of electron waves which includes both remote and near scattering.

III. WAVE-OPTICAL APPROACH TO LOCAL INTERFERENCE

The wave-optical approach to local interference to be presented in this section starts from the assumption of a homogeneous distribution of elastic scatterers and from an arbitrary number of such scatterers involved in trajectories which take part in the interference. It turns out that to describe the conductance fluctuations due to local interference only three types of combinations of backscattered trajectories, involving at most two scatterers, need to be considered. These types of combinations are (i) two remote trajectories, (ii) two near trajectories, and (iii) one remote and one near trajectory. For a homogeneous distribution of scatterers, however, these combinations do not lead to agreement with the experimental data. Such an agreement is found by taking into account enhanced scattering in the constriction region, again for the combination of one remote and one near trajectory. This situation is equivalent to a shorter elastic mean free path in the constriction region and characterizes the special scattering conditions in our point contacts, as discussed in detail at the end of this section.

A. General formulation

To describe local interference of electron waves for the point-contact situation, we consider trajectories starting at the orifice and returning to it after several elastic-scattering processes. The initial states $\psi_{\mathbf{k}}(\mathbf{0})$ in the contact region are the wave functions of the ballistic problem. In the experiments[1,2,4] the inequality $ka \gg 1$ is satisfied, so that the initial states are described very accurately by plane waves of wave vector $\mathbf{k}$. At large distances from the orifice, however, the states are not plane waves due to diffraction at the orifice.[16] As a result of diffraction, considerable phase differences can occur between waves arriving at point $\mathbf{R}$ from different positions at the orifice. For $R < R_d \equiv ka^2$ diffraction can be neglected,[16] so that for each $\mathbf{k}$ one deals with a "geometrical beam" of constant width $2a$ in the direction of $\mathbf{k}$. For this range, the wave-function amplitude is the same as at the orifice, i.e., $|\psi_{\mathbf{k}}(\mathbf{0})|$. At distances $R > R_d$ diffraction should be considered, so that the wave function amplitude decreases according to

$$|\psi_{\mathbf{k}}| \approx |\psi_{\mathbf{k}}(\mathbf{0})| \frac{ka^2}{R} . \tag{2}$$

The divergence angle of the diffraction cone is $\approx 1/ka$, so that in this range the beam width increases by a factor R/ka^2 with respect to its geometrical size. This corresponds to the main diffraction maximum. For directions

far from $\mathbf{k}$, which corresponds to the side diffraction maxima, one obtains

$$|\psi_{\mathbf{k}}| \approx |\psi_{\mathbf{k}}(0)| \frac{a}{R\,(ka)^{1/2}} \ . \tag{3}$$

For the point contacts we consider, R_d is about 1000 nm. Since the thickness of the banks is 200–250 nm, we are always in the range of the geometrical beam.

To calculate the amplitude of the fluctuations, we start from the expression for the interference contribution to the backscattered current, relative to the incident current:

$$W_{\rm int} = \frac{\left| \sum\limits_{\mathbf{k}=\mathbf{k}_F} \int d^2r [\psi_{\mathbf{k},b}(r) \nabla \psi^*_{\mathbf{k},b'}(\mathbf{r}) - \psi^*_{\mathbf{k},b}(\mathbf{r}) \nabla \psi_{\mathbf{k},b'}(\mathbf{r})] \right|}{\pi a^2 \left| \sum\limits_{\substack{\mathbf{k}=\mathbf{k}_F \\ k_x>0}} \mathbf{k} \psi_{\mathbf{k}}(0) \right|^2} \ . \tag{4}$$

Here, the vector $\mathbf{r}$ ($r \le a$) is the 2D radius vector in the plane of the orifice. The functions $\psi_{\mathbf{k},b}(\mathbf{r})$ and $\psi_{\mathbf{k},b'}(\mathbf{r})$ are wave functions at the orifice, which result from backscattering (denoted by b and b') along any possible backscattered trajectories, i.e., along trajectories involving any possible number of scatterers:

$$\psi_{\mathbf{k},b}(\mathbf{r}) = \sum_{\{n\}} \frac{\psi_{\mathbf{k}}(\mathbf{R}_1) F_1 F_2 \cdots F_n \exp[ik(|\mathbf{R}_2-\mathbf{R}_1| + |\mathbf{R}_3-\mathbf{R}_2| + \cdots + |\mathbf{r}-\mathbf{R}_n|)]}{|\mathbf{R}_2-\mathbf{R}_1||\mathbf{R}_3-\mathbf{R}_2| \cdots |\mathbf{r}-\mathbf{R}_n|} \ . \tag{5}$$

In Eq. (5) $\mathbf{R}_1, \mathbf{R}_2, \ldots, \mathbf{R}_n$ are scatterer coordinates, $F_1, F_2, \ldots, F_n$ are scattering amplitudes, which are taken as $F = (\sigma/4\pi)^{1/2}$ for all scatterers, and the summation $\{n\}$ is over all possible numbers of scatterers n involved in the backscattered trajectories. In Eq. (5) we assume that the spacing between successive scattering processes does not exceed l_e. Figure 3 schematically depicts three possible backscattered trajectories, involving one, two, or three scatterers.

From Eqs. (4), (5) one obtains the following expression for $W_{\rm int}$ due to trajectories involving n and n' scatterers:

$$W_{\rm int} = \sum_{\mathbf{k}=\mathbf{k}_F} \sum_{\{n\}\{n'\}} W_{\mathbf{k}}(\mathbf{R}_1, \mathbf{R}_2, \ldots, \mathbf{R}_n; \mathbf{R}_{1'}, \mathbf{R}_{2'}, \ldots, \mathbf{R}_{n'}) \ . \tag{6a}$$

Here, $W_{\mathbf{k}}$ is given by

$$\begin{aligned} &W_{\mathbf{k}}(\mathbf{R}_1, \mathbf{R}_2, \ldots, \mathbf{R}_n; \mathbf{R}_{1'}, \mathbf{R}_{2'}, \ldots, \mathbf{R}_{n'}) \\ &= \frac{2}{\sum\limits_{\mathbf{k}=\mathbf{k}_F} |\psi_{\mathbf{k}}(0)|^2 \pi a^2} \int d^2r \left(\frac{\sigma}{4\pi} \right)^{(n+n')/2} |\psi_{\mathbf{k}}(\mathbf{R}_1)||\psi_{\mathbf{k}}(\mathbf{R}_{1'})| \\ &\quad \times \frac{\cos[k(|\mathbf{R}_2-\mathbf{R}_1| + \cdots |\mathbf{r}-\mathbf{R}_n| - |\mathbf{R}_{2'}-\mathbf{R}_{1'}| - \cdots - |\mathbf{r}-\mathbf{R}_{n'}|) + \mathbf{k}\cdot(\mathbf{R}_1-\mathbf{R}_{1'})]}{|\mathbf{R}_2-\mathbf{R}_1| \cdots |\mathbf{r}-\mathbf{R}_n||\mathbf{R}_{2'}-\mathbf{R}_{1'}| \cdots |\mathbf{r}-\mathbf{R}_{n'}|} \\ &\quad \times \left[\mathbf{e}_1 \cdot \left[\frac{\mathbf{r}-\mathbf{R}_n}{|\mathbf{r}-\mathbf{R}_n|} + \frac{\mathbf{r}-\mathbf{R}_{n'}}{|\mathbf{r}-\mathbf{R}_{n'}|} \right] \right] \ . \end{aligned} \tag{6b}$$

As before, $\{n\}$ and $\{n'\}$ in Eq. (6a) run over all possible numbers of scatterers n and n' involved in the trajectories. $\mathbf{e}_1$ is a unit vector in the positive x direction normal to the plane of the orifice (see Fig. 3). In deriving Eq. (6b) only the dominating contribution of the exponential of the spherical waves to the gradients was retained.

Since the average of $W_{\rm int}$ over defect positions vanishes, the magnitude of the conductance fluctuations should be obtained from the mean quadratic interference contribution:

$$\frac{\delta G}{G} = \sqrt{\langle W_{\rm int}^2 \rangle} \ . \tag{7}$$

Here, the ensemble average $\langle W_{\rm int}^2 \rangle$ is given by

$$\langle W_{\rm int}^2 \rangle = \sum_{\mathbf{k}=\mathbf{k}_F} \sum_{\{n\}\{n'\}} \int d\mathbf{R}_1 \cdots d\mathbf{R}_n d\mathbf{R}_{1'} \cdots d\mathbf{R}_{n'} N_i^{(n+n')} W_{\mathbf{k}}^2(\mathbf{R}_1, \ldots, \mathbf{R}_n; \mathbf{R}_{1'}, \ldots, \mathbf{R}_{n'}) \ . \tag{8}$$

In Eq. (8) the density of scatterers N_i is supposed to be homogeneous, as in Sec. II A. Further, the interval of integration over positions of the initial scatterers at $\mathbf{R}_1$ and $\mathbf{R}_{1'}$ is $[0, l_e]$, which depending on the relative magnitude of R_d and l_e can include both the geometrical beam region ($R_1, R_{1'} < R_d$), where $|\psi_{\mathbf{k}}(\mathbf{R})| = |\psi_{\mathbf{k}}(0)|$ and $\int d\mathbf{R}(\cdots) \to \int \pi a^2 dR(\cdots)$, and the main diffraction maximum region ($R_1, R_{1'} > R_d$), where according to Eq.

(2) $|\psi_{\mathbf{k}}(\mathbf{R})| = |\psi_{\mathbf{k}}(\mathbf{0})| ka^2/R$ and where $\int d\mathbf{R}(\cdots) \rightarrow \int R^2 dR\, d\Omega(\cdots)$. In the last case, $\mathbf{R}$ is limited to a diffraction cone of solid angle $1/(ka)^2$, which determines $\int d\Omega$. Integration over positions of other scatterers can obviously be converted to $\int R^2 dR\, d\Omega(\cdots)$, which is limited to a half space. From further analysis of Eqs. (6), (8), it can be concluded that (i) for trajectories with more than one scatterer the main contribution to $\langle W_{\text{int}}^2 \rangle$ comes from remote scatterers at distance l_e, and (ii) addition of a scatterer to such a trajectory does not contribute to $\langle W_{\text{int}}^2 \rangle$, since it leads to an additional factor $N_i \sigma \int R_i^2 dR_i d\Omega / |\mathbf{R}_j - \mathbf{R}_i|^2 \approx 1$ (where it was used that $l_e = 1/N_i\sigma$).

The definition of the magnitude of the conductance fluctuations given in Eqs. (7), (8) supposes that the contributions of different $\mathbf{k}$ modes propagating through the contact are uncorrelated. Actually, some correlation of the contributions of different $\mathbf{k}$ modes exists for a special choice of the trajectories. In Appendix A it will be shown, however, that this correlation is of no importance in our case.

One might expect that the main contribution to $\langle W_{\text{int}}^2 \rangle$ comes from "diffusive" trajectories with many scatterers (as for UCF). For the point-contact situation, however, the importance of such trajectories is reduced as a result of their small return probability. Apart from this, for ballistic point contacts the contribution of long trajectories is suppressed by inelastic processes, due to the nonzero temperature or an applied bias.

B. Limit of a small number of scatterers: Combination of near and remote backscattered trajectories

The arguments at the end of the previous section allow us to reduce the problem "in zeroth order" to that of trajectories involving at most two scatterers, which is the smallest number necessary to form a loop of area $\approx l_e^2$ with the starting and ending points in the constriction region. First, we analyze the case that *both trajectories* forming the loop each involve *two scatterers*. This means that in Eq. (6a), we only consider the term with $n = n' = 2$:

$$\langle W_{\text{int}}^2 \rangle = \sum_{\mathbf{k}=\mathbf{k}_F} \int d\mathbf{R}_1 d\mathbf{R}_2 d\mathbf{R}_{1'} d\mathbf{R}_{2'} N_i^4 \times W_k^2(\mathbf{R}_1, \mathbf{R}_2; \mathbf{R}_{1'}, \mathbf{R}_{2'}) \,. \tag{9}$$

Further, the integration over $\mathbf{r}$ in Eq. (6b) reduces to

$$I = \int d\mathbf{r} \frac{\cos\{k[|\mathbf{r}-\mathbf{R}_2| - |\mathbf{r}-\mathbf{R}_{2'}| + \Gamma(\mathbf{R}_1, \mathbf{R}_2, \mathbf{R}_{1'}, \mathbf{R}_{2'})]\}}{|\mathbf{r}-\mathbf{R}_2||\mathbf{r}-\mathbf{R}_{2'}|} \times \left[\mathbf{e}_1 \cdot \left(\frac{\mathbf{r}-\mathbf{R}_2}{|\mathbf{r}-\mathbf{R}_2|} + \frac{\mathbf{r}-\mathbf{R}_{2'}}{|\mathbf{r}-\mathbf{R}_{2'}|} \right) \right] . \tag{10}$$

Here, $\Gamma(\mathbf{R}_1, \mathbf{R}_2, \mathbf{R}_{1'}, \mathbf{R}_{2'})$ includes the $\mathbf{r}$-independent terms of the argument of the cosine. It can be shown (see Appendix B) that only in two special cases the integral Eq. (10) takes a substantial value. These two cases occur either when the straight line connecting $\mathbf{R}_2$ and $\mathbf{R}_{2'}$ hits the orifice, while $R_{\min} = \min(R_2, R_{2'}) < R_d$, or when both $\mathbf{R}_2$ and $\mathbf{R}_{2'} (R_2, R_{2'} > R_d)$ are inside the same diffraction cone (see Fig. 4). The value of the integral for the two cases is summarized by

$$I \approx \frac{1}{k} \frac{\pi}{R_2 R_{2'}} \min(R_d, R_{\min}) \,. \tag{11}$$

In the experiments R_d exceeds l_e, so that the relevant situation is defined by $R_1, R_{1'}, R_2, R_{2'} < R_d$. For this situation, we obtain the fluctuation amplitude (see Appendix C)

$$\delta G = \sqrt{\langle W_{\text{int}}^2 \rangle}\, G \approx \frac{\sqrt{6}}{8} \frac{a^2}{l_e^2} \frac{e^2}{h} \,, \tag{12}$$

where in addition to the contribution of the transmitted electron flux (to which the description was limited so far) also the contribution of the incident electron flux has been taken into account (see Appendix C). The estimate Eq. (12) is identical to the one discussed in Sec. II B. This is as expected, since Eq. (12) was derived for the same ballistic situation as assumed in Ref. 7: a clean near region and a low density of scatterers in the diffusive remote region. Since two remote trajectories are involved in this estimate, the corresponding B_c value has the proper magnitude.

Another possibility to be considered is that *one trajectory* includes *two scatterers*, while *the other* includes only *one scatterer*, i.e., $n = 2, n' = 1$. In this case, $\mathbf{R}_{1'}$ should be in the common volume of the geometrical beam and the cone from $\mathbf{R}_2$ towards the orifice. This means that the single scatterer should be relatively close to the constriction. In the estimate for δG, this is expressed by taking the interval of integration for $R_{1'}$ as $[0, a]$ along the direction of the geometrical beam. As a result, one obtains for δG a gain of a factor $(l_e/a)^{1/2}$ with respect to Eq. (12), resulting in (see Appendix C)

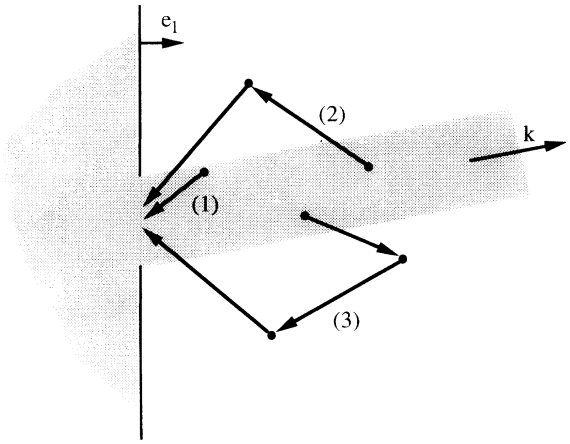

FIG. 3. Typical backscattered trajectories relevant for interference. The shaded area to the right of the orifice is the transmitted geometrical beam. Trajectory (1) represents near scattering involving one scatterer in the constriction region, while trajectories (2) and (3) are remoted backscattered trajectories involving two and three scatterers, respectively. For trajectories (2) and (3), the typical distance between successive scattering events is l_e, while the first and last scattering event is also within a distance l_e of the orifice.

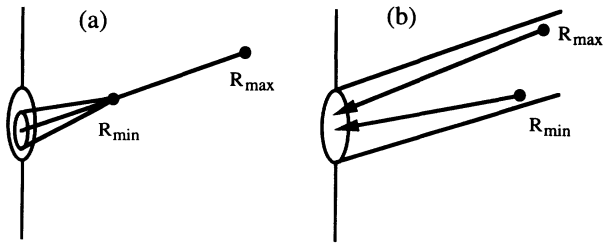

FIG. 4. The two special situations are depicted, which contribute to the interference effect. In scattering geometry (a) the straight line connecting the last scatterer of the two trajectories hits the orifice, while $R_{min} < R_d$. The top angle of the cone extending from $\mathbf{R}_{min}$ towards the orifice is $(kR_{min})^{-1/2}$. In scattering geometry (b) the two last scatterers are outside the sphere of radius R_d and inside the same diffraction cone.

$$\delta G \approx \frac{\sqrt{3}}{2}\left[\frac{a}{l_e}\right]^{3/2}\frac{e^2}{h} . \tag{13}$$

This estimate for combined near and remote scattering is still smaller by a factor $(a/l_e)^{1/2}$ than the experimentally observed δG. Since there is one remote trajectory involved, the B_c value corresponding to this estimate has the proper magnitude.

As an obvious further step, we consider the case that *both trajectories* involved in the interference contain *one scatterer* (i.e., $n = n' = 1$). This provides an even larger gain of a factor (l_e/a) with respect to Eq. (12). In Appendix C we derive for this situation

$$\delta G \approx \frac{2\sqrt{2}}{7}\frac{a}{l_e}\frac{e^2}{h} . \tag{14}$$

This result derived for backscattering controlled by only near scatterers is identical to Eq. (1) derived in Sec. II A from the Landauer formula. The inadequacy of the magnetic-field scale corresponding to this estimate to explain the experimental results was already discussed in Sec. II A.

In our local interference model presented up to here, a homogeneous distribution of scatterers was assumed throughout the point contact. However, it is likely that enhanced scattering will occur in the constriction region as a result of strain due to thermal stresses and as a result of boundary scattering. In Eq. (8) this inhomogeneous scattering can be taken into account as an increased effective defect concentration $N_{i,c}$ in the immediate constriction region, corresponding to a mean free path $l_{e,c}$ around the constriction which is smaller than in the banks. This is not contradictory to the high-quality point-contact spectra which can be taken from the devices,[1,17] since in many cases this does not indicate more than that the ratio $l_{e,c}/a$ has a value larger than two or three,[18,19] while no information about the real defect concentration can be obtained. For the case $n = 2, n' = 1$ the introduction of the quantity $N_{i,c}$ leads to a gain of a factor $(l_e^2/a l_{e,c})^{1/2}$ compared to Eq. (12) (see Appendix C). So, for δG, we get

TABLE I. A summary is given of combinations of backscattered trajectories giving rise to conductance fluctuations due to interference of electron waves. Prefactors of δG were omitted. The dashed constriction region in the lower right geometry indicates enhanced near scattering.

No. of scatt. traject. 1	2 (remote)	1 (near)	1 (near)	1 (near, enh.)
No. of scatt. traject. 2	2 (remote)	2 (remote)	1 (near)	2 (remote)
$\delta G(e^2/h)$	$\left[\frac{a}{l_e}\right]^2$	$\left[\frac{a}{l_e}\right]^{3/2}$	$\frac{a}{l_e}$	$\frac{a}{l_e}\left[\frac{a}{l_{e,c}}\right]^{1/2}$
$B_c(T)$	$\frac{h/e}{l_e^2}$	$\frac{h/e}{l_e^2}$	$\frac{h/e}{a^2}$	$\frac{h/e}{l_e^2}$
geometry of traject.	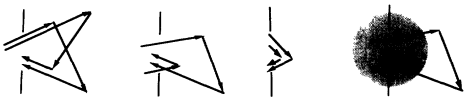			

$$\delta G \approx \frac{\sqrt{3}}{2}\left[\frac{a}{l_{e,c}}\right]^{1/2}\frac{a}{l_e}\frac{e^2}{h} . \tag{15}$$

Again, because one remote trajectory is part of the interference loop, the B_c value corresponding to this estimate has the proper magnitude. One expects that $l_{e,c}$ scales with a ($l_{e,c} \geq a$), so that Eq. (15) effectively is the same estimate as Eq. (1). The upper estimate for δG results for $l_{e,c} \approx a$. This will, for instance, hold in case of effective boundary scattering, which can easily occur. The reason is that the actual constriction geometry will always deviate from a hole in an insulating layer of zero thickness, in spite of marginal breakthrough of the nitride membrane during etching (see also Ref. 5). In Table I, we summarize the estimates for δG and B_c for the various cases discussed in this section.

Quantitatively, if we assume enhanced scattering in the constriction region for the point contacts of Fig. 1 ($l_{e,c} \approx a$), Eq. (15) leads to the estimates δG_{theo} compiled in Table II, which also gives other characteristics of these devices. As can be seen from the table, the theoretical estimates are in very good agreement with the experimental values. As a further support of our theory, we mention that experiments on Ag, Au, and Al point contacts,[4,20] including those of Fig. 1, show that δG indeed scales with a/l_e, while the product $B_c l_e^2$ in units h/e is a constant of

TABLE II. Characteristics of the conductance fluctuations of Fig. 1. Entries in the table are the contact resistance R, the contact radius a, the elastic mean free path l_e of the banks, the experimental (theoretical) values of the fluctuation amplitude $\delta G_{exp(theo)}$, and, finally, the experimental (theoretical) values of the characteristic field scale $B_{c,exp(theo)}$.

Contact	R (Ω)	a (nm)	l_e (nm)	δG_{exp} (e^2/h)	δG_{theo} (e^2/h)	$B_{c,exp}$ (T)	$B_{c,theo}$ (T)
Ag	11	5.8	240	0.023	0.021	0.13	0.08
Au	7.5	7.0	190	0.029	0.032	0.29	0.13
Al	16	3.3	48	0.024	0.060	0.13	2.0

order unity.

In our considerations of the fluctuations so far, the characteristic field scale B_c was directly estimated from the typical loop size for each specific combination of trajectories. A more formal way is to derive B_c from the correlation function of the fluctuations, which is defined as $F(\Delta B)=\langle W_{\rm int}(B)W_{\rm int}(B+\Delta B)\rangle$. For the relevant case $n=2, n'=1, F(\Delta B)$ is proportional to

$$\int d\mathbf{R}_1 d\mathbf{R}_2 \frac{\cos\left[\chi(\mathbf{R}_1,\mathbf{R}_2)+2\pi\frac{\Phi(\mathbf{R}_1,\mathbf{R}_2)}{h/e}\right]\cos\left[\chi(\mathbf{R}_1,\mathbf{R}_2)+2\pi\frac{\Phi(\mathbf{R}_1,\mathbf{R}_2)}{h/e}+2\pi\frac{\Delta\Phi(\mathbf{R}_1,\mathbf{R}_2)}{h/e}\right]}{|\mathbf{R}_1-\mathbf{R}_2|^2 R_2^2} . \tag{16}$$

Here, $\chi(\mathbf{R}_1,\mathbf{R}_2)$ is a phase at $B=0$ and $\Phi(\mathbf{R}_1,\mathbf{R}_2)$ is the magnetic flux through the loop formed by the positions of the scatterers and the orifice, which for the large spatial scales in question can be considered as a point. To make a rough estimate of $F(\Delta B)$, we transform coordinates as in Appendix C, take as the upper integration limit for R_1 and R_2 the elastic mean free path l_e, make the approximation $|\mathbf{R}_1-\mathbf{R}_2|^{-2}\approx 3l_e^{-2}$ (see Appendix C) and $\Phi\approx BR_1R_2/2$ and rewrite the product of cosines to a sum of cosines [noting that the resulting integral with $\chi(\mathbf{R}_1,\mathbf{R}_2)$ in the argument of the cosine vanishes]. So we obtain

$$F(\Delta B)\propto\int_0^{l_e}dR_1\int_0^{l_e}dR_2\cos\left[\frac{\pi\Delta BR_1R_2}{h/e}\right]$$
$$\approx\frac{h/e}{\pi\Delta B}\mathrm{Si}\left[\frac{\pi\Delta Bl_e^2}{h/e}\right], \tag{17}$$

where $\mathrm{Si}(x)$ is the sine integral, obeying $\mathrm{Si}(0)=0$ and $\mathrm{Si}(x\to\infty)=\pi/2$. The characteristic field scale of the fluctuations is defined as the field B_c for which $F(B_c)=F(0)/2$. From Eq. (17), it can be found that $B_c=1.2(h/e)/l_e^2$, in agreement with our previous conclusions.[1,2,4] From Table II we observe that for the Ag and Au point contacts $B_{c,\rm exp}$ and $B_{c,\rm theo}$ agree well. That for these contacts $B_{c,\rm theo}$ is somewhat low may be due to loop areas being smaller than $R_1R_2/2$ and the plane of the loops not being perpendicular to magnetic field. For Al $B_{c,\rm theo}$ is high, consistent with $\delta G_{\rm theo}$ being relatively high. The origin of this discrepancy is not clear, but it may be due to the value $\rho l_e=4\times10^{-16}\ \Omega\,\mathrm{m}^2$ used in calculating a and l_e of the Al contact. The literature values of ρl_e cover a wide range, and choosing ρl_e in the upper part of this range would give a better agreement. In Fig. 5, the theoretical function $F_{\rm theo}$ given by Eq. (17) is compared with the experimental function $F_{\rm exp}$ of the 11-Ω Ag point contact. As can be seen from the figure, $F_{\rm theo}$ globally has all the features of $F_{\rm exp}$. In detail, however, there are some differences, the most salient difference occurring for $\Delta B<B_c$. In this range, $F_{\rm exp}$ (thought to be symmetric around $\Delta B=0$) is like a sharp peak and is clearly smaller than $F_{\rm theo}$. We speculate that this behavior of $F_{\rm exp}$, which has also been found for several other contacts,[4] arises from an additional contribution of interference loops which involve more scatterers than the simple loops which lead to Eq. (17) and which thus lead to smaller characteristic field scales. The effect of such loops will be discussed elsewhere.

The key results of this section, Eqs. (15), (17) and the property that the corresponding $B_c=1.2(h/e)/l_e^2$, have been derived in the framework of a qualitatively new physical picture, which gives a consistent description of the fluctuation amplitude and the magnetic-field scale. Ingredients in the physical picture which are new compared to those of Refs. 1, 7 are (i) a wave-optical approach to local interference, (ii) both near and remote scattering, (iii) interference due to the combination of near and remote backscattered trajectories, and (iv) enhanced scattering strength near the constriction.

The local-interference theory of the conductance fluctuations described above has several important advantages. First, being transparent and straightforward, it provides a simple physical picture, but nevertheless has the versatility to take into account many details (such as interference of waves propagating along different types of trajectories or a nonhomogeneous distribution of scatterers) which are not so easy to describe by more formal procedures. Second, it provides the necessary ingredients for numerical simulations of quantum interference in ballistic metallic point contacts.

To conclude this section, we note that the magnetoconductance in addition to the fluctuations also demonstrates

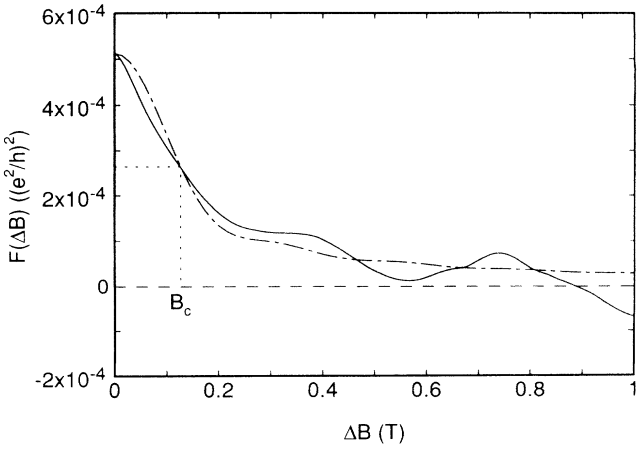

FIG. 5. The solid line is the correlation function of the fluctuations of the 11-Ω Ag point contact of Fig. 1. The dashed line is the theoretical function given in Eq. (17), which was made to coincide with the experimental function at $\Delta B=0$ and at $\Delta B=B_c$.

a systematic behavior: a positive magnetoconductance for fields up to several Tesla and a negative magnetoconductance beyond this range. For the traces in Fig. 1(a) this effect is most pronounced for the Au point contact. It can be shown that the negative magnetoconductance is due to bending of classical electron trajectories in the contact region, while the positive magnetoconductance possibly arises from weak localization involving, in particular, interference of remote and near trajectories. We will discuss these phenomena in more detail elsewhere.[21]

IV. SUMMARY AND CONCLUSIONS

In summary, we have developed a theory for conductance fluctuation in ballistic metallic point contacts, using general wave optics to describe the propagation of electrons in the devices. In our approach, the conductance fluctuations originate from local interference of electron waves elastically backscattered to the constriction. Due to the "diffusivelike" nature of the electron paths, only backscattered trajectories involving at most two scatterers need to be taken into account.

As limiting cases of our theory, we can reproduce the estimates of δG of Refs. 1 and 7, which demonstrates the universality of our approach. These estimates, however, which are mutually contradictory and do not properly describe the experiments of Refs. 1,2,4, were derived either for dominating near scattering or for dominating remote scattering, respectively. In real devices, on the contrary, both near and remote backscattered trajectories simultaneously play a role in the interference. By combining these two types of trajectories and by making the additional assumption of enhanced scattering in the constriction region (of which the origin probably is boundary scattering), we find very good quantitative agreement with the experiments, both for δG and B_c, thus lifting the previous contradictions. This agreement is achieved by calculating the enhancement of δG (compared to the case of only remote trajectories[7]) due to the larger return probability of trajectories confined to the near region, while backscattered trajectories spreading out to the remote regions are responsible for the magnetic-field scale.

The property that the fluctuation amplitude depends on the local elastic mean free path can, in principle, be used to probe the scattering strength close to the constriction, for example by deriving $l_{e,c}$ as a fit parameter. In this way it is possible to obtain information on the actual contact realization which is not accessible using other methods.

In spite of the larger return probability of near trajectories, we find that the most probable *loops* contributing to the effect involve one remote trajectory. This also means that the fluctuation amplitude will not be larger at higher magnetic fields (where smaller loops are probed), not even at the fields corresponding to loops confined in the contact region. This agrees with the experimental result.[1,2,4]

ACKNOWLEDGMENT

V. I. Kozub gratefully acknowledges the "Nederlandse Organisatie voor Wetenschappelijk Onderzoek (NWO)" for a visitors grant.

APPENDIX A

As discussed in Sec. III A, there exists a correlation of contributions of different $\mathbf{k}$ modes for a special choice of the trajectories. This can be demonstrated by considering pairs of trajectories (inside the half-sphere of radius R_d) which, apart from the condition that the line connecting the last scatterers at $\mathbf{R}_n$ and $\mathbf{R}_{n'}$ should hit the orifice, also obey this condition for the initial scatterers at $\mathbf{R}_1$ and $\mathbf{R}_{1'}$. This condition for the relative positions of the last scatterers is just the general condition to provide a substantial contribution to the interference (see Appendix B). The condition for the relative positions of the initial scatterers clearly is stronger than the simple condition of being in the same geometrical beam and implies a reduction of the phase volume available for the initial scatterers. Initial modes $\mathbf{k}$ and $\mathbf{k}'$ parallel to, respectively, the lines connecting $\mathbf{R}_1,\mathbf{R}_{1'}$ and $\mathbf{R}_n,\mathbf{R}_{n'}$ satisfy the relations

$$\mathbf{k}\cdot(\mathbf{R}_1-\mathbf{R}_{1'})=k|\mathbf{R}_1-\mathbf{R}_{1'}|\alpha(\mathbf{R}_1,\mathbf{R}_{1'}) \tag{A1a}$$

and

$$\mathbf{k}'\cdot(\mathbf{R}_n-\mathbf{R}_{n'})=k'|\mathbf{R}_n-\mathbf{R}_{n'}|\alpha(\mathbf{R}_n,\mathbf{R}_{n'}) , \tag{A1b}$$

where $\alpha(\mathbf{R}_i,\mathbf{R}_{i'})=\mathrm{sgn}[\mathbf{e}_1\cdot(\mathbf{R}_i-\mathbf{R}_{i'})]$ indicates the ordering with respect to the orifice of the scatterers at $\mathbf{R}_i,\mathbf{R}_{i'}$. The correlation can be identified by considering the cosine in the integrand of Eq. (6b). The integration over $\mathbf{r}$ in Eq. (6b) reduces the contribution of the cosine to its value corresponding to a slow variation of the phase $k(|\mathbf{r}-\mathbf{R}_n|-|\mathbf{r}-\mathbf{R}_{n'}|)$. Consequently, we can write

$$k(|\mathbf{r}-\mathbf{R}_n|-|\mathbf{r}-\mathbf{R}_{n'}|)\approx k|\mathbf{R}_n-\mathbf{R}_{n'}|\alpha(\mathbf{R}_n,\mathbf{R}_{n'}) . \tag{A2}$$

If Eqs. (A1), (A2) hold it follows that traversal of trajectories $(\mathbf{R}_1,\mathbf{R}_2,\ldots,\mathbf{R}_n)$ and $(\mathbf{R}_{1'},\mathbf{R}_{2'},\ldots,\mathbf{R}_{n'})$ by a wave related to initial mode $\mathbf{k}$ yields the same value of the cosine as traversal of the same trajectories traversed in the opposite direction by a wave related to initial mode $\mathbf{k}'$ ($k'=k=k_F$). This correlation is obviously related to the well-known contribution of the particle-particle (Cooper) channel to UCF.[3] In this sense, the contribution given by Eq. (8) in Sec. III B arises from the particle-hole channel. The contribution of the particle-particle channel is given by

$$\langle W^2_{\mathrm{int},p-p}\rangle=\sum_{\mathbf{k}=\mathbf{k}_F}\sum_{\mathbf{k}'=\mathbf{k}_F}\sum_{\{n\}\{n'\}}\int d\mathbf{R}_1\cdots d\mathbf{R}_n d\mathbf{R}_{1'}\cdots d\mathbf{R}_{n'}N_i^{(n+n')}$$

$$\times W_{\mathbf{k}}(\mathbf{R}_1,\ldots,\mathbf{R}_n;\mathbf{R}_{1'},\ldots,\mathbf{R}_{n'})W_{\mathbf{k}'}(\mathbf{R}_n,\ldots,\mathbf{R}_1;\mathbf{R}_{n'},\ldots,\mathbf{R}_{1'}) . \tag{A3}$$

As a result of Eqs. (A1a), (A1b) the phase volume available for the initial and last scatterers is restricted according to the inequalities

$$|\mathbf{k}\cdot(\mathbf{R}_1-\mathbf{R}_{1'})-k|\mathbf{R}_1-\mathbf{R}_{1'}|\alpha(\mathbf{R}_1,\mathbf{R}_{1'})| \ll \pi \qquad \text{(A4a)}$$

and

$$|\mathbf{k}'\cdot(\mathbf{R}_n-\mathbf{R}_{n'})-k'|\mathbf{R}_n-\mathbf{R}_{n'}|\alpha(\mathbf{R}_n,\mathbf{R}_{n'}| \ll \pi\ , \qquad \text{(A4b)}$$

which allows the wave vectors $\mathbf{k}$ and $\mathbf{k}'$ to slightly deviate from being parallel to the vectors $\mathbf{R}_1-\mathbf{R}_{1'}$ and $\mathbf{R}_n-\mathbf{R}_{n'}$, respectively. It can be shown, by applying phase volume arguments of the type also used in Appendix B, that Eqs. (A4) leads to a reduction of the total phase volume for the initial and last scatterers by a factor $\approx(ka)^{-2}$ compared to the situation for the particle-hole channel. However, in Eq. (A3) there is an additional summation over the modes $\mathbf{k}'$ for each given mode $\mathbf{k}$, which gives an additional factor $\approx(ka)^2$. As a result, for the special pairs of trajectories defined by Eqs. (A4), the contribution of the particle-particle channel is equal to that of the particle-hole channel, and it thus doubles the mean quadratic fluctuation amplitude. However, due to reversed ordering of the scatterers for the particle-particle channel, the magnetic flux contribution enters the arguments of the cosines in Eq. (16) with opposite signs, so that the contribution of this channel is already suppressed at a moderate field, as is also known for UCF.[3] Since in the experiments the applied fields are much larger than this field, we have not taken into account the contribution of the particle-particle channel to the fluctuation amplitude.

APPENDIX B

In this appendix, we derive Eq. (11) of Sec. III B. As a starting point, we repeat Eq. (10):

$$I=\int d\mathbf{r}\frac{\cos\{k[|\mathbf{r}-\mathbf{R}_2|-|\mathbf{r}-\mathbf{R}_{2'}|+\Gamma(\mathbf{R}_1,\mathbf{R}_2,\mathbf{R}_{1'},\mathbf{R}_{2'})]\}}{|\mathbf{r}-\mathbf{R}_2||\mathbf{r}-\mathbf{R}_{2'}|}\left[\mathbf{e}_1\cdot\left[\frac{\mathbf{r}-\mathbf{R}_2}{|\mathbf{r}-\mathbf{R}_2|}+\frac{\mathbf{r}-\mathbf{R}_{2'}}{|\mathbf{r}-\mathbf{R}_{2'}|}\right]\right]\ . \qquad \text{(B1)}$$

In general, the cosine in the integrand of Eq. (B1) is a rapidly oscillating function of $\mathbf{r}$ across the area of the orifice. This consequently causes the integral to average to a small value. In two special cases, however, a substantial part of the orifice is an area of virtually constant phase difference for waves emitted from $\mathbf{R}_2$ and $\mathbf{R}_{2'}$, so that the cosine varies slowly in that part. These two cases occur (see Fig. 4) either when the straight line connecting $\mathbf{R}_2$ and $\mathbf{R}_{2'}$ hits the orifice, while $R_{\min}=\min(R_2,R_{2'})<R_d$, or when both $\mathbf{R}_2$ and $\mathbf{R}_{2'}$ $(R_2,R_{2'}>R_d)$ are inside the same diffraction cone. In the former case the area of constant phase is given by the intersection with the orifice of a cone having its top at $\mathbf{R}_{\min}$. This cone is defined by

$$\angle(\mathbf{r}-\mathbf{R}_{\min},\mathbf{R}_{\min}-\mathbf{R}_{2'})\le\frac{1}{\sqrt{kR_{\min}}}\ , \qquad \text{(B2)}$$

where $\angle(\mathbf{a},\mathbf{b})$ denotes the angle between the vectors $\mathbf{a}$ and $\mathbf{b}$. The available phase volume for $\mathbf{R}_{\min}$ is inside the solid angle $\pi a^2(1/R_2-1/R_{2'})^2$, which is determined by the cone extending from $\mathbf{R}_{\max}$ to the orifice ($\mathbf{R}_{\max}$ is the longer vector of $\mathbf{R}_2,\mathbf{R}_{2'}$). In the latter case the whole orifice is an area of constant phase. The question what is the phase volume for $\mathbf{R}_{\min}$, subject to the condition that the path difference $|\mathbf{r}-\mathbf{R}_2|-|\mathbf{r}-\mathbf{R}_{2'}|$ should be virtually constant across the whole orifice, is equivalent to the question, what are the possible directions for waves emitted by the orifice in the direction of $\mathbf{R}_{\max}$, such that they also arrive in phase at $\mathbf{R}_{\min}$. From diffraction theory, it is known that these directions are inside a diffraction cone of solid angle $1/(ka)^2$ centered around the direction of $\mathbf{R}_{\max}$. For the value of the integral given in Eq. (B1), these considerations lead to

$$I\approx\frac{1}{k}\frac{\pi}{R_2R_{2'}}\min(R_d,R_{\min})\ , \qquad \text{(B3)}$$

which is Eq. (11) of Sec. III B. In Eq. (B3), we have omitted the numerator of the integrand, being the value of the cosine in the area of constant phase difference, and the factor involving scalar products with $\mathbf{e}_1$, which factor is a slowly varying function of $\mathbf{r}$. For our purpose this omission is justified, since these functions enter Eq. (9) squared, so that a weighing is carried out by a function of effective value of order unity. The restriction of the phase volume for $R_{\min}$ obviously leads to a decrease of the phase volume of trajectories contributing to Eq. (9), since it restricts the integration over the coordinate of the last scatterer in each arm. The restriction leads to a reduction of the integral Eq. (9) by a factor

$$\tfrac{1}{2}a^2\left[\frac{1}{R_2}-\frac{1}{R_{2'}}\right]^2 \quad \text{for } R_{\min}<R_d\ , \qquad \text{(B4a)}$$

and

$$\frac{1}{2\pi(ka)^2} \quad \text{for } R_{\min}>R_d\ . \qquad \text{(B4b)}$$

In situations other than the special cases the rapid oscillations of the integrand average to zero, except in a narrow band at the circumference of the orifice. For the narrow band, one finds from statistical arguments,

$$I\approx\frac{a^2}{R_2R_{2'}}\frac{1}{ka}\frac{1}{\sqrt{ka}}\ . \qquad \text{(B5)}$$

The square of the ratio of estimates Eq. (B3), (B5) yields a factor $(ka)^3\min(1,R_{\min}^2/R_d^2)$. This factor multiplied by the reduction factors in Eqs. (B4a), (B4b) equals

$ka(1-R_{\min}/R_{\max})^2/2$ for $R_{\min}<R_d$ or $ka/2\pi$ for $R_{\min}>R_d$. The latter result certainly is much larger than unity, while the former result, in general, also will be larger than unity, except in the case $R_{\min}/R_{\max}\approx 1$. Realizations for which this occurs are rare, in view of the average distance between the scatterers and the conditions imposed on their relative positions. So, in general, the decrease of phase volume described by Eqs. (B4) is strongly compensated for by the magnitude of the integral given in Eq. (B3). Thus, pairs of trajectories leading to the estimate given in Eq. (B3) make the dominant contribution to the effect. This also holds for cases other than $n=n'=2$ (see Appendix C).

APPENDIX C

In this Appendix, we make the estimates of the fluctuation amplitude δG presented in Sec. III B. To this end, we first note that according to Eqs. (4), (8) $\langle W_{\rm int}^2\rangle$ originates from backscattering of electron channels initially transmitted through the orifice. However, one can also consider the complementary problem of elastic scattering of the electron flux incident towards the orifice. In a way similar to that of the transmitted flux, this gives an interference contribution to the current through the contact, which is independent of the contribution of the transmitted flux. This contribution results from interference of waves which after one or more collisions are scattered into a $\mathbf{k}$ mode of the constriction, which subsequently is transmitted. The contribution of the incident flux to $\langle W_{\rm int}^2\rangle$ is equal to that of the transmitted flux, so that in this appendix $\langle W_{\rm int}^2\rangle$ has a magnitude which is twice that of Eq. (8).

We start with the case that both trajectories involve two scatterers, i.e., $n=n'=2$. From Eq. (6b), we have

$$W_k=\frac{\sigma^2}{8\pi^3a^2\sum\limits_{\mathbf{k}=\mathbf{k}_F}|\psi_{\mathbf{k}}(0)|^2}\times\frac{|\psi_{\mathbf{k}}(\mathbf{R}_1)||\psi_{\mathbf{k}}(\mathbf{R}_{1'})|I(\mathbf{R}_1,\mathbf{R}_2,\mathbf{R}_{1'},\mathbf{R}_{2'})}{|\mathbf{R}_2-\mathbf{R}_1||\mathbf{R}_{2'}-\mathbf{R}_{1'}|}\ , \tag{C1}$$

where $I(\mathbf{R}_1,\mathbf{R}_2,\mathbf{R}_{1'},\mathbf{R}_{2'})$ is the integral given in Eq. (B1). Equation (C1) can be reduced by noting that $|\psi_{\mathbf{k}}(\mathbf{R}_1)|=|\psi_{\mathbf{k}}(\mathbf{R}_{1'})|=|\psi_{\mathbf{k}}(0)|$ for $R_1,R_{1'}<R_d$, while $\sum_{k=k_F}1=a^2k_F^2/4$ and according to Eq. (B3) $I(\mathbf{R}_1,\mathbf{R}_2,\mathbf{R}_{1'},\mathbf{R}_{2'})\approx 1/(kR_{2'})$ for the choice $R_2=R_{\min}$. So we get

$$W_k\approx\frac{\sigma^2}{2\pi^3a^4k^3}\frac{\pi}{|\mathbf{R}_2-\mathbf{R}_1||\mathbf{R}_{2'}-\mathbf{R}_{1'}|R_{2'}}\ . \tag{C2}$$

Since for the case of local interference discussed here, one has $R_1,R_2,R_{1'},R_{2'}\le l_e$, the upper limits of the integrals of Eqs. (8), (9) are set to l_e. Thus, by combining Eq. (9) and Eq. (C2), it follows

$$\begin{aligned}\langle W_{\rm int}^2\rangle&=2\sum_{\mathbf{k}=\mathbf{k}_F}\int d\mathbf{R}_1d\mathbf{R}_2d\mathbf{R}_{1'}d\mathbf{R}_{2'}N_i^4W_{\mathbf{k}}^2(\mathbf{R}_1,\mathbf{R}_2;\mathbf{R}_{1'},\mathbf{R}_{2'})\\&=\frac{1}{8\pi^4l_e^4a^6k^4}\int_{R_1=0}^{R_1=l_e}\frac{d\mathbf{R}_1}{|\mathbf{R}_2-\mathbf{R}_1|^2}\int_{R_{1'}=0}^{R_{1'}=l_e}\frac{d\mathbf{R}_{1'}}{|\mathbf{R}_{2'}-\mathbf{R}_{1'}|^2}\int_{R_2=0}^{R_2=l_e}d\mathbf{R}_2\int_{R_{2'}=R_2}^{R_{2'}=l_e}\frac{d\mathbf{R}_{2'}}{R_{2'}^2}\ .\end{aligned} \tag{C3}$$

To arrive at Eq. (C3), it was used that the summation over k states at the Fermi surface again just yields the number of channels propagating through the contact. We proceed by making the approximation $|\mathbf{R}_2-\mathbf{R}_1|^{-2}\approx|\mathbf{R}_{2'}-\mathbf{R}_{1'}|^{-2}\approx 3l_e^{-2}$ (which corresponds to an average of these quantities over a sphere of radius l_e) and by transforming to spherical and cylindrical coordinates. Actually, for the integration over positions $\mathbf{R}_1$ and $\mathbf{R}_{1'}$ elliptical coordinates should be used. However, the difference between the two types of coordinates is only pronounced for $\mathbf{k}$ directions far from the axis of the point contact, which justifies our choice. From Appendix B, we use $\int d\Omega_2=\pi a^2(1/R_2-1/R_{2'})^2$. Finally, we get

$$\begin{aligned}\langle W_{\rm int}^2\rangle&\approx\frac{1}{4l_e^4k^4}\int_0^{l_e}\frac{dR_1}{|\mathbf{R}_2-\mathbf{R}_1|^2}\int_0^{l_e}\frac{dR_{1'}}{|\mathbf{R}_{2'}-\mathbf{R}_{1'}|^2}\int_0^{l_e}dR_2R_2^2\int_{R_2}^{l_e}dR_{2'}\left[\frac{1}{R_2}-\frac{1}{R_{2'}}\right]^2\\&\approx\frac{1}{4l_e^4k^4}\frac{3l_e}{l_e^2}\frac{3l_e}{l_e^2}\frac{l_e^2}{6}\\&=\frac{6}{256}\frac{a^4}{l_e^4}\frac{16}{(ka)^4}\ .\end{aligned} \tag{C4}$$

From this we find, using Eq. (7)

$$\delta G\approx\frac{\sqrt{6}}{8}\frac{a^2}{l_e^2}\frac{e^2}{h}\ . \tag{C5}$$

The next case to consider is $n=2,n'=1$. For the choice $R_{1'}=R_{\min}$, we get

$$W_{\mathbf{k}}=\frac{8\sigma^{3/2}}{(4\pi)^{3/2}\pi a^4k^3}\frac{\pi}{|\mathbf{R}_2-\mathbf{R}_1|R_2}\ , \tag{C6}$$

$$\langle W_{\rm int}^2\rangle = 2\sum_{\mathbf{k}=\mathbf{k}_F}\int d\mathbf{R}_1 d\mathbf{R}_2 d\mathbf{R}_{1'} N_i^3 W_k^2(\mathbf{R}_1,\mathbf{R}_2;R_{1'})$$
$$= \frac{1}{2\pi^3 l_e^3 a^6 k^4}\int_{R_{1'}=0}^{R_{1'}=a} d\mathbf{R}_{1'}\int_{R_1=0}^{R_1=l_e}\frac{d\mathbf{R}_1}{|\mathbf{R}_2-\mathbf{R}_1|^2}\int_{R_2=R_{1'}}^{R_2=l_e}\frac{d\mathbf{R}_2}{R_2^2}\ . \tag{C7}$$

As discussed in Sec. III B, the requirement that the line connection $\mathbf{R}_{1'}$ and $\mathbf{R}_2$ should hit the orifice, can to a good approximation be taken into account by integrating R_1 over the interval $[0,a]$ along the direction of the geometrical beam. Again changing the integration variables, we get

$$\langle W_{\rm int}^2\rangle \approx \frac{1}{2\pi l_e^3 a^2 k^4}\int_0^{l_e}\frac{dR_1}{|\mathbf{R}_2-\mathbf{R}_1|^2}\int_0^a dR_{1'}\int_{R_{1'}}^{l_e}$$
$$\times dR_2\int d\Omega_2$$
$$\approx \frac{1}{2\pi l_e^3 a^2 k^4}\frac{3l_e}{l_e^2}(l_e a-\tfrac{1}{2}a^2)2\pi$$
$$\approx \frac{3}{16}\frac{a^3}{l_e^3}\frac{16}{(ka)^4}\ . \tag{C8}$$

From this we find

$$\delta G \approx \frac{\sqrt{3}}{2}\left[\frac{a}{l_e}\right]^{3/2}\frac{e^2}{h}\ . \tag{C9}$$

For $n=2,n'=1$ it is also possible to consider the situation $R_2=R_{\rm min}$. This will reduce the fluctuation amplitude below the value of Eq. (C9), since the probability to backscatter to the orifice from position $\mathbf{R}_{1'}$ will be reduced. Since Eq. (B9) already gives a too low estimate, we will not consider this possibility.

Now we consider the case $n=1,n'=1$. For the choice $R_1=R_{\rm min}$, we get

$$W_k = \frac{2\sigma}{\pi^2 a^4 k^3}\frac{\pi}{R_{1'}}\ , \tag{C10}$$

$$\langle W_{\rm int}^2\rangle = 2\sum_{\mathbf{k}=\mathbf{k}_F}\int d\mathbf{R}_1 d\mathbf{R}_{1'} N_i^2 W_k^2(\mathbf{R}_1;\mathbf{R}_{1'})$$
$$= \frac{2}{\pi^2 l_e^2 a^6 k^4}\int_{R_1=0}^{R_1=l_e} d\mathbf{R}_1\int_{R_{1'}=R_1}^{R_{1'}=l_e}\frac{d\mathbf{R}_{1'}}{R_{1'}^2}$$
$$= \frac{2}{l_e^2 a^2 k^4}\int_0^{l_e} R_1^2 dR_1\int_{R_1}^{l_e} dR_{1'}\left[\frac{1}{R_1}-\frac{1}{R_{1'}}\right]^2\frac{1}{R_{1'}^2}$$
$$= \frac{2}{48}\frac{a^2}{l_e^2}\frac{16}{(ka)^4}\left[\ln\left[\frac{l_e}{a}\right]-\frac{33}{18}\right]\ . \tag{C11}$$

To arrive at the last expression of Eq. (C11), we have lifted the divergency of the integration over R_1 by introducing "by hand" the contact radius a as the lower integration limit. This seems a logical choice, since for our experiments the radius is in the range $(0-0.16)l_e$, as required by the last factor in Eq. (C11), and since it is not in contradiction with the homogeneous distribution of scatterers assumed for this case. Since in the experiments $[\ln(l_e/a)-\frac{33}{18}]\approx 1$, we find from Eq. (C11)

$$\delta G \approx \frac{2\sqrt{2}}{7}\frac{a}{l_e}\frac{e^2}{h}\ . \tag{C12}$$

Finally, we consider the case $n=2,n'=1$ under the condition of enhanced scattering in the constriction region. This is due to an effective density of elastic scattering centers $N_{i,c}$ in the constriction region which is larger than in the remote regions. Taking into account $N_{i,c}$ leads to a modified version of Eq. (C8), which involves $l_{e,c}=(\sigma N_{i,c})^{-1}$:

$$\langle W_{\rm int}^2\rangle = \frac{3}{16}\frac{a^3}{l_{e,c}l_e^2}\frac{16}{(ka)^4}\ . \tag{C13}$$

From this we find

$$\delta G \approx \frac{\sqrt{3}}{2}\left[\frac{a}{l_{e,c}}\right]^{1/2}\frac{a}{l_e}\frac{e^2}{h}\ . \tag{C14}$$

*Permanent address: A. F. Ioffe Physico-Technical Institute, 194021, St. Petersburg, Russia.
†Present address: Shell Research/KSEPL, Volmerlaan 6, 2288 GD Rijswijk, The Netherlands.

[1]P. A. M. Holweg, J. A. Kokkedee, J. Caro, A. H. Verbruggen, S. Radelaar, A. G. M. Jansen, and P. Wyder, Phys. Rev. Lett. **67**, 2549 (1991).
[2]P. A. M. Holweg, J. Caro, A. H. Verbruggen, and S. Radelaar, Phys. Rev. B **48**, 2479 (1993).
[3]P. A. Lee, A. D. Stone, and H. Fukuyama, Phys. Rev. B **35**, 1039 (1987).
[4]P. A. M. Holweg, Ph.D. thesis, Delft University of Technology, 1992.
[5]P. A. M. Holweg, J. Caro, A. H. Verbruggen, and S. Radelaar, Microelectron. Eng. **11**, 27 (1990).
[6]P. A. Lee, Physica **140A**, 169 (1986).

[7]D. L. Maslov, C. Barnes, and G. Kirczenov, Phys. Rev. Lett. **70**, 1984 (1993).
[8]J. W. Martin, Philos. Mag. **24**, 555 (1971).
[9]J. Pelz and J. Clarke, Phys. Rev. B **36**, 4479 (1987).
[10]Yu. M. Galperin and V. I. Kozub. Zh. Eksp. Teor. Fiz. **100**, 323 (1991) [Sov. Phys. JETP **73**, 179 (1991)].
[11]P. H. M. van Loosdrecht *et al.*, Phys. Rev. B **38**, 10 162 (1988).
[12]L. I. Glazman and M. Jonson, Phys. Rev. B **41**, 10 686 (1990); **44**, 3810 (1991).
[13]C. Beenakker and H. van Houten in Solid State Phys. **44**, (1991).
[14]R. Landauer, Philos. Mag. **21**, 863 (1970).
[15]G. Wexler, Proc. Phys. Soc. London **89**, 927 (1966).
[16]In this section we apply general considerations of diffraction of electron waves at an orifice, which for light waves in some form can be found in text books, for example M. Born and E. Wolf, *Principles of Optics* (Pergamon Press, New York, 1975).
[17]P. A. M. Holweg, J. Caro, A. H. Verbruggen, and S. Radelaar, Phys. Rev. B **45**, 9311 (1992).
[18]I. O. Kulik, R. I. Shekhter, and A. G. Shkorbatov, Zh. Eksp. Teor. Fiz. **81**, 2126 (1981) [Sov. Phys. JETP **54**, 1130 (1981)].
[19]A. I. Akimenko, A. B. Verkin, N. M. Ponomarenko, and I. K. Yanson, Fiz. Nizk. Temp. **8**, 260 (1982) [Sov. J. Low Temp. Phys. **8**, 130 (1982)].
[20]P. A. M. Holweg *et al.* (unpublished).
[21]J. Caro *et al.* (unpublished).

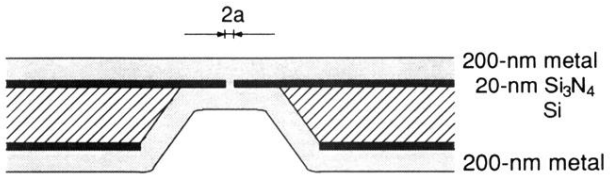

FIG. 2. Schematic cross section of a nanofabricated point contact. The diameter $2a$ of a typical point contact is in the range 5–30 nm.

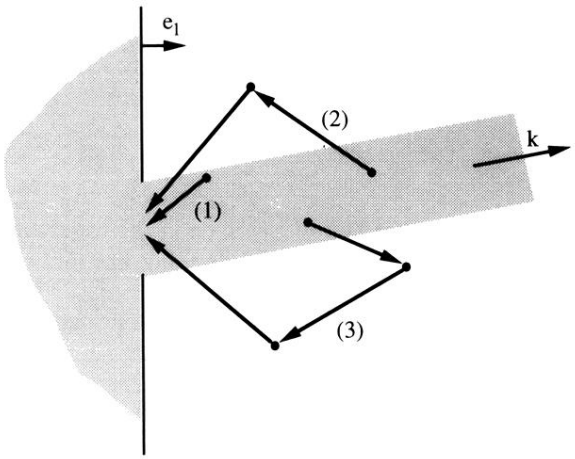

FIG. 3. Typical backscattered trajectories relevant for interference. The shaded area to the right of the orifice is the transmitted geometrical beam. Trajectory (1) represents near scattering involving one scatterer in the constriction region, while trajectories (2) and (3) are remoted backscattered trajectories involving two and three scatterers, respectively. For trajectories (2) and (3), the typical distance between successive scattering events is l_e, while the first and last scattering event is also within a distance l_e of the orifice.